Biochemical and Biophysical Research Communications 370 (2008) 195–199

Contents lists available at ScienceDirect

Biochemical and Biophysical Research Communications

journal homepage: www.elsevier.com/locate/ybbrc

SSA/Ro52 autoantigen interacts with Dcp2 to enhance its decapping activity

Tadanori Yamochi, Kei Ohnuma, Osamu Hosono, Hirotoshi Tanaka, Yoshiyuki Kanai, Chikao Morimoto *

Department of Clinical Immunology, Advanced Clinical Research Center, Institute of Medical Science, University of Tokyo, 4-6-1, Shirokanedai, Minato-ku, Tokyo 108-8639, Japan

ARTICLE INFO

Article history:
Received 10 March 2008
Available online 24 March 2008

Keywords:
Autoantigen
Autoantibody
Ro52
Decapping enzyme
hDCP2
mRNA decay
p-bodies

ABSTRACT

We identified human decapping enzyme 2 (hDCP2) as a binding protein with Ro52, being colocalized in processing bodies (p-bodies). We also showed that the N-terminus and C-terminus of Ro52 bound to hDCP2. Moreover, Ro52 enhanced decapping activity of hDCP2 in a dose-dependent manner. Our data support the novel notion of the association between Ro52 with hDCP2 protein in cytoplasmic p-bodies, playing a role in mRNA metabolism in response to cellular stimulation.

A member of TRIM (Tripartite motif family), Ro52 is a component of a group of SS-A/Ro autoantigens, which is composed of at least a 60 kDa (Ro60) protein, a 52 kDa protein (Ro52-α), and a 45 kDa protein (Ro52-β) [1–6] The TRIM proteins including Ro52 appear to play a role in such functions as development and cell growth, and TRIM proteins show specific localization such as a discrete speckled pattern in the nucleus or cytoplasm [5]. In human, autoantibodies to the SS-A/Ro autoantigens are commonly found in the sera of patients with autoimmune diseases such as systematic lupus erythematosus (SLE), Sjögren's syndrome (SjS), neonatal lupus erythematosus/congenital heart block, and primary biliary cirrhosis (PBC) [7–9]. We previously demonstrated that anti-CD28 mAb enhanced IL-2 production of Ro52 Jurkat transfectant and changed the intracellular localization of Ro52 in a cytoplasmic discrete speckled pattern [10]. However, the molecular mechanism involved in Ro52 subcellular translocation is unknown, and proteins interacting with Ro52 in the cytoplasmic discrete speckled pattern are undefined.

The human autoantigen Gw-182 is located in p-bodies and has an important role in mRNA decay [11–13], and sera containing autoantibody to Ro52 from patients with SjS are reported to react with the p-bodies [13,14]. Furthermore, the proteins involved in the 5′–3′ decay pathway are concentrated in cytoplasmic discrete speckled patterns named mRNA "processing bodies" (p-bodies) [15–21]. In p-bodies, human DCP2 (hDCP2) appears to play a central role in mRNA decay by its decapping enzyme activity [22], via its interaction with human DCP1 (hDCP1), Ge-1/hedls, Dhh1, and EDC3 [16,23]. In the study using clinical samples, 44% of patients with anti-p-bodies (Gw-182) had reactivity to Ro52 [14]. This observation suggests that Ro 52 is one of target in patients with anti-p-bodies autoantibody. However, it has not yet been confirmed whether Ro52 is a functional component of p-bodies, or is a bystander. Putting together these findings and our previous observation that Ro52 proteins are localized in p-bodies-like discrete speckled pattern, we hypothesized that Ro52 protein may be associated with p-bodies and have a functional role in mRNA decapping.

In the present study, we used biochemical assays to demonstrate that Ro52 protein is associated with hDCP2. We found that both the N-terminal and the C-terminal domains of Ro52 protein are required for its binding to hDCP2, while both Box A and Box B domains of the latter are required for its binding to Ro52. Furthermore, we showed that Ro52 enhances the decapping activity of hDCP2 in a dose-dependent manner of Ro52. Our results therefore imply that Ro52 is a key regulatory of mRNA decay via positively regulating the catalytic activity of hDCP2.

Materials and methods

Constructions of plasmids. The plasmid pEGFP-hDCP2 (kindly provided by Dr. Bertrand Seraphin at Center National de la Recherche Scientifique) was used. GST-hDCP2, 6xHis-hDCP2, Azami-hDCP2 were made by inserting hDCP2 cDNA into mammalian GST expression vector pEBG (28), pCold (TAKARA), Azami (MBL), and pEGFP (BD Clontech), respectively. GST-Ro52, JRed, and Ro52-GFP were made by inserting Ro52 cDNA into pEBG, JRed (Evrogen), and pEGFP (BD Clontech). N-termi-

* Corresponding author. Fax: +81 364 092 098.
E-mail address: morimoto@ims.u-tokyo.ac.jp (C. Morimoto).

0006-291X/$ - see front matter © 2008 Elsevier Inc. All rights reserved.
doi:10.1016/j.bbrc.2008.03.075

nally BioEase-tagged hDCP2 was constructed using Invitrogen Gateway technology (Invitrogen). A series of hDCP2 or Ro52 deletion mutants were made by inserting cDNA fragments of mutated hDCP2 or Ro52 generated by the polymerase chain reaction (PCR) into pEBG Vector. All constructs and cDNA were confirmed by DNA sequencing.

Purification and detection of biotin–hDCP2 binding proteins GST pull-down assay. To produce BioEase-tagged hDCP2, we used NativePure mammalian Affinity Purification kit (Invitrogen) according to the manufacturer's instructions. Briefly, the plasmid constructs were transfected into 293 FT cells. Cells were lysed with lysis buffer and lysates were pulled down by streptavidin agarose beads. To remove the BioEase Tag, the pulled down beads were cleaved by AcTEV protease, and the supernatant was concentrated by Microcon YM30.

GST fusion proteins were produced and pull-down assays were performed as previously described [24,25].

Production of recombinant protein. To produce 6xHis-hDCP2, the plasmid constructs were transformed into BL21 (DE3); pT-Trx *Escherichia coli* [24]. The recombinant proteins were purified on a nickel column (QIAGEN) under denaturing conditions with 8 M urea according to the manufacturer's instructions. Purified protein was renatured by refolding CA kit (TAKARA). Renatured protein was dialyzed with storage buffer (10 mM Tris–HCl, pH 7.9, 100 mM NaCl, 2 mM MG-Ac, 1 mM DTT, and 10% glycerol).

In vitro decapping assays. A $5'^{m7}$ cap labeled RNA substrate was produced by incubating 304 nucleotide T7 β-actin RNA transcript with [α-^{32}P]GTP, S-adenosyl-L-methionine(Ambion) and vaccinia virus capping enzyme. Decapping reactions were carried out at 30 °C for 1 h in a total of 20 μl of 50 mM Tris–HCl (pH8.0)–30 mM $(NH_4)_2SO_4$–1 mM $MgCl_2$ containing ~30 nCi of cap labeled RNA and recombinant hDCP2. All reactions were terminated by the addition of EDTA to 10 mM, and 5 μl was separated by thin-layer chromatography (TLC).

Results

Interaction of Ro52 with hDCP2

It has been reported that Ro52 localized to "dot-like" structures in the cytoplasm [26]. We also previously reported that Ro52 was localized in a "dot-like" cytoplasmic discrete speckled pattern following Jurkat-T cell stimulation [10]. Other investigators have showed that patient sera with reactivity to p-bodies were identified as the cytoplasmic discrete speckled pattern observed by indirect immunofluorescence [27], suggesting that Ro52 may be involved in p-bodies. In p-bodies, hDCP2 is found to be a key subunit of the decapping enzyme complex [28]. Accordingly, to evaluate the possibilities that Ro52 is in p-bodies, we first analyzed the subcellular localization of an ectopically expressed Green Fluorescence Protein, Azami tagged with hDCP2 (Azami-DCP2) and/or Red Fluorescence Protein, JRed tagged with Ro52 (Ro52-JRed). As

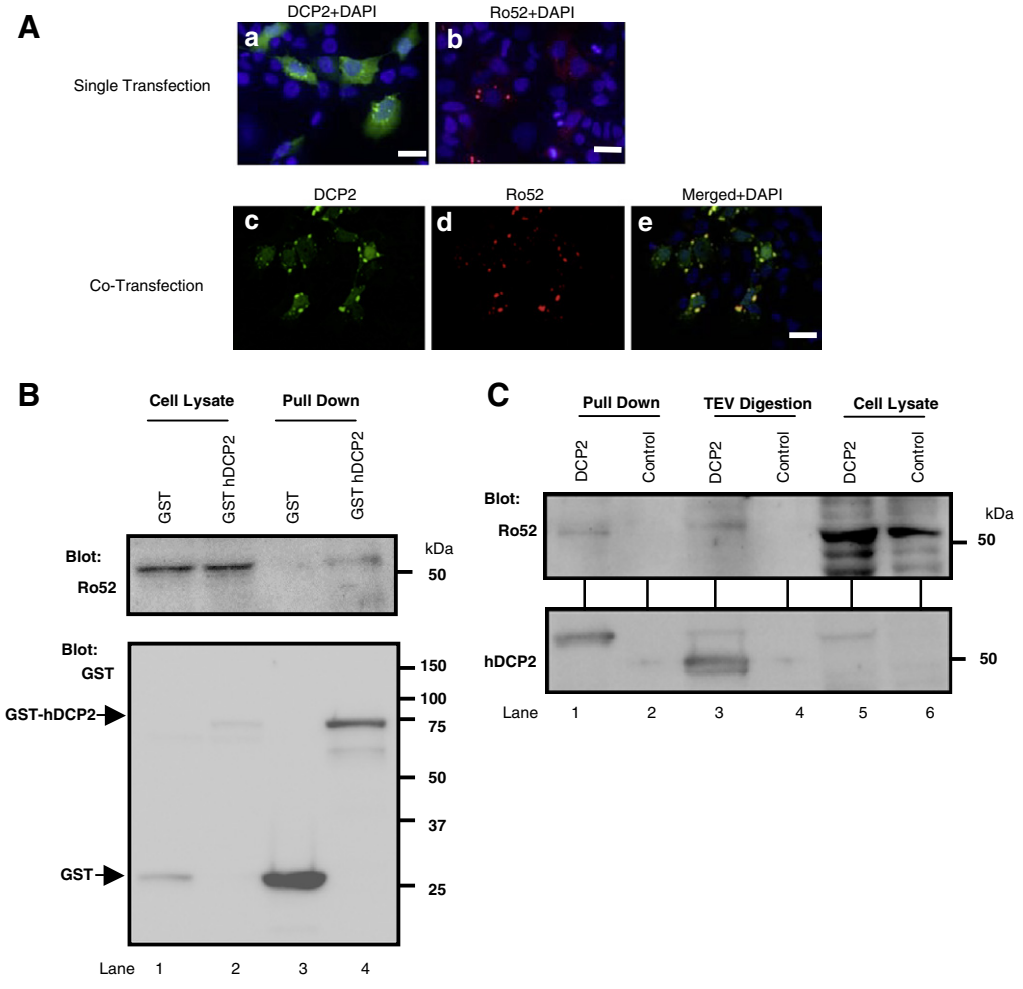

Fig. 1. Binding of Ro52 to hDCP2. (A) (a) 293FT cells were transfected with Azami hDCP2 (green) and stained with DAPI. (b) 293FT cells were transfected with Ro52-JRed (red). (c–e) Azami-hDCP2(green) and Ro52-JRed (red) were cotransfected into 293FT cells. The cells were examined for nuclear DNA (DAPI), Azami-hDCP2 and Ro52-JRed. Bars indicate a 20-μm scale. (B) Following transfection of 293 FT cells with GST alone (lanes 1 and 3) or GST-hDCP2 (lanes 2 and 4), cell lysates were prepared as described in Materials and methods. 10% total cell lysate (lanes 1 and 2), and pulled down GST-beads using total cell lysates (lanes 3 and 4) were separated using 10% SDS–PAGE, and immunoblotted with anti-Ro52 mAb (upper panel), followed by stripping and reprobing with anti-GST pAb (lower panel). (C) Following transfection of 293 FT cells with BioEase-tagged hDCP2 (lanes 1, 3, and 5) or Vector alone (lanes 2, 4, and 6), cell lysates were prepared as described in Materials and methods. Lanes 1 and 2: streptavidin beads pulled down using total cell lysates. Lanes 3 and 4: Concentrated elute of protein complex cleaved by AcTEV Enzyme. Lanes 5 and 6: 10% total cell lysates. The treated samples were separated using 10% SDS–PAGE, and immunoblotted with anti-Ro52 pAb (upper panel), followed by stripping and reprobing with anti-DCP2 pAb (lower panel). (For interpretation of color mentioned in this figure the reader is referred to the web version of the article.)

shown in Fig. 1A, Azami-hDCP2 was observed in cytoplasmic discrete speckled patterns (a), as reported previously [28] and Ro52-JRed showed several discrete speckled patterns in the cytoplasm (b). Following cotransfection of JRed Ro52 and Azami hDCP2, JRed Ro52 was demonstrated to merge with Azami hDCP2 in a discrete speckled pattern (c–e of Fig. 1). These results hence suggested that Ro52 is associated with hDCP2 in p-bodies.

Next, we conducted GST pull-down assay using GST-fused hDCP2 protein (GST-hDCP2) expressed in mammalian cells. As shown in Fig. 1B, endogenous Ro52 was coprecipitated with GST-hDCP2 (lane 4 of upper panel), but not with GST alone (lane 3 of upper panel). This association between endogenous Ro52 and hDCP2 was confirmed by using BioEase-tagged hDCP2 (bio-hDCP2) as another conjugated hDCP2 protein in a biotin pull-down system with avidin beads (Fig. 1C). Meanwhile, Ro52 was coprecipitated with bio-hDCP2 (lane 1 in upper panel of Fig. 1C) but not with Bio-Ease mock alone (lane 2 of upper panel of Fig. 1C). Furthermore, to exclude the possibility of nonspecific binding of Ro52 to the avidin beads, hDCP2 protein complex was eluted with cleavage by AcTEV enzyme. Ro52 was detected in the complex of hDCP2 elutes (lane 3 of upper panel of Fig. 1C), but not in the elutes of mock transfected cells (lane 4 in upper panel of Fig. 1C). These data suggested that Ro52 binds to hDCP2 in *in vivo* and *in vitro* conditions.

Identification of binding domain of Ro52 with hDCP2

We next determined the binding domains involved in the Ro52-hDCP2 interaction through a series of GST-fused Ro52 or hDCP2 and their deletion mutants (Fig. 2A). A series of GST-fused Ro52 and its deletion mutants were cotransfected with Flag-tagged hDCP2 WT. As shown in the right panel of Fig. 2B, coprecipitation assay with glutathione beads showed that Flag-tagged hDCP2 was coprecipitated with GST Ro WT (lane 9 of upper panel), Ro-N terminal region (RoN) (lane 6 of upper panel), or Ro-C terminal region (RoC) (lane 8 of upper panel) but not with GST Ro-Coiled Coil region (RoCC) (lane 7 of upper panel) or GST alone (lane 10 of upper panel). These results suggested that N- and CT-terminal regions of Ro52 were required for its binding to hDCP2.

The binding domain of hDCP2 to Ro52 was then determined using a series of GST-fused hDCP2 and its deletion mutant. As shown in the right panel of Fig. 2C, Ro52 was coprecipitated with GST-hDCP2 WT (lane 6 of upper panel), hDCP2N (lane 7 of upper panel), and hDCP2 C (lane 9 of upper panel) but not with GST-hDCP2 94–259 AAs (lane 8 of upper panel) and GST alone (lane 10 of upper panel), data implying that 1–93 amino acids and C-terminal region of hDCP2 were required for binding to Ro52.

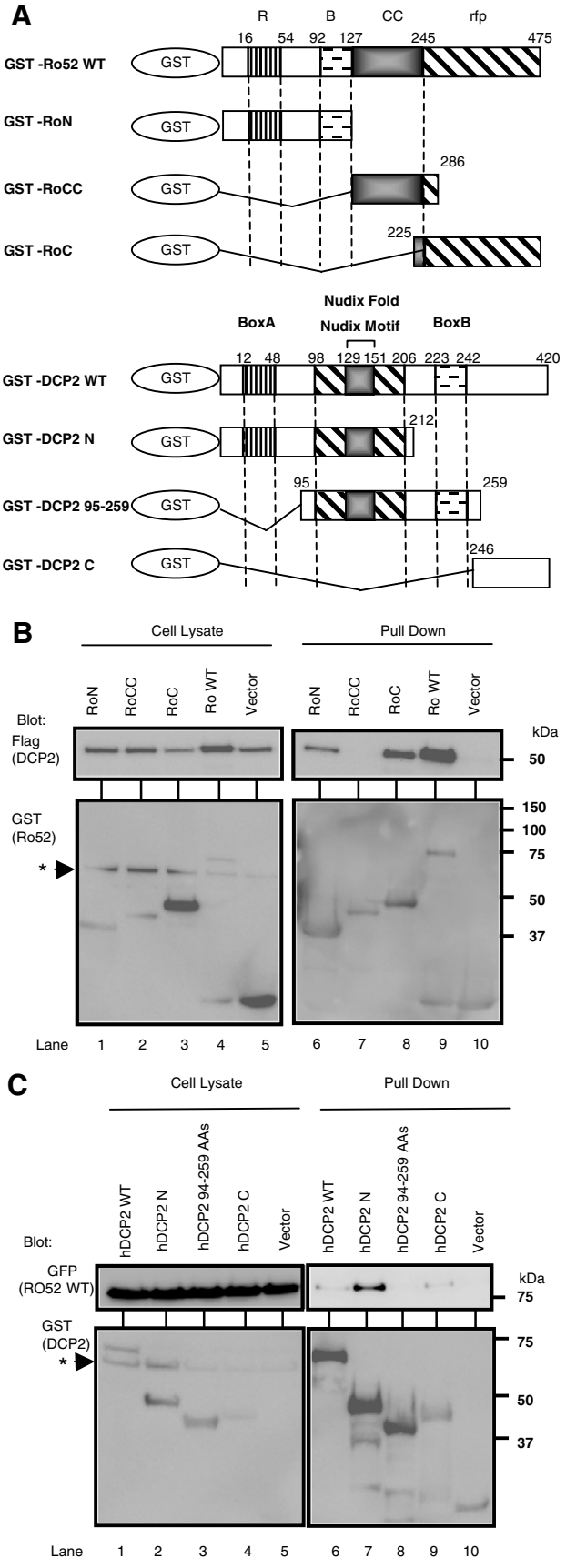

Fig. 2. Determination of the binding domains involved in the interaction between Ro52 and hDCP2. (A) Schematic representation of GST-Ro52 or hDCP2 and their deletion mutants. In Ro52, Residues 16–54 comprised the Ring Finger Domain (R) (Vertically striped square), residues 92–127 comprised the B Box Domain (B) (Horizontal striped square), residues 128–245 comprised the Coiled Coil Domain (CC) (Black square), residues 246–475 comprised the Rfp Domain (Striped square). In hDCP2, residues 12–48 comprised the BoxA Domain (BoxA) (Vertically striped square), residues 98–206 comprised the Nudix Fold Domain (Nudix Fold) (Striped square) with the central residues 129–151 being the Nudix motif (Nudix Motif) (Blacked square), residues 223–242 comprised the BoxB Domain (BoxB) (Horizontal striped square). (B) Following transfection of 293 FT cells with Flag-hDCP2 and GST-Ro52 or its deletion mutants, cell lysates were prepared as described in Materials and methods and pulled down by glutathione beads. One percent of total cell lysates (lanes 1–5) and the pulled down beads (lanes 6–10) were separated using 10% SDS–PAGE, and immunoblotted with anti-GFP mAb (upper panel), followed by stripping and reprobing with anti-GST pAb (lower panel). *Nonspecific bands. (C) Determination of binding domain of hDCP2 to Ro52. 293 FT cells were transfected with GFP-Ro52 and GST-hDCP2 or its deletion mutants. One percent of total cell lysates (lanes 1–5) and the pulled down beads (lanes 6–10) were separated using 10% SDS–PAGE, and immunoblotted with anti-Flag mAb (upper panel), followed by stripping and reprobing with anti-GST mAb (lower panel). *Nonspecific bands.

Decapping activity of hDCP2 is enhanced by its interaction with Ro52

It has been reported that hDCP2 plays a central role in mRNA decay by its decapping enzyme activity [22]. We therefore examined the potential effect of Ro52 on hDCP2 decapping activity through *in vitro* decapping assay. Native form of hDCP2 was constructed and purified as described in Materials and methods. As shown in Fig. 3A, purified recombinant hDCP2 protein was capable of decapping the capped RNA and releasing m^7GDP product in a dose-dependent manner (lanes 2 and 3). Of note was that this decapping activity of purified hDCP2 was inhibited by the addition of EDTA (lane 4), implying that hDCP2 may be appropriate for use in *in vitro* decapping assay as reported previously [29]. Using this recombinant hDCP2 proteins, we next examined the effect of Ro52 on hDCP2 activity with the use of Flag-tagged Ro52 and two other deletion mutants involving Ro52 ΔCC and Ro52 CC (Fig. 3B). As shown in Fig. 3C, the addition of Ro52WT enhanced hDCP2 decapping activity in a dose-dependent manner (lanes 1–3). Similarly, the addition of Ro52 ΔCC, capable of binding to hDCP2 (as shown in Fig. 2B), also enhanced decapping activities (lanes 4–6 in Fig. 3C). However, the addition of Ro52 CC, which did not bind to hDCP2 (as shown in Fig. 2B), did not result in enhanced decapping activity as compared with Ro52 WT (lanes 7–9 in Fig. 3C). Likewise, decapping activity was not observed with purified Ro52 proteins alone, in the absence of hDCP2 (data not shown). These results suggested that the interaction between Ro52 and hDCP2 can affect decapping activity of hDCP2 *in vitro*, and that Ro52 has a potential role in mRNA decay.

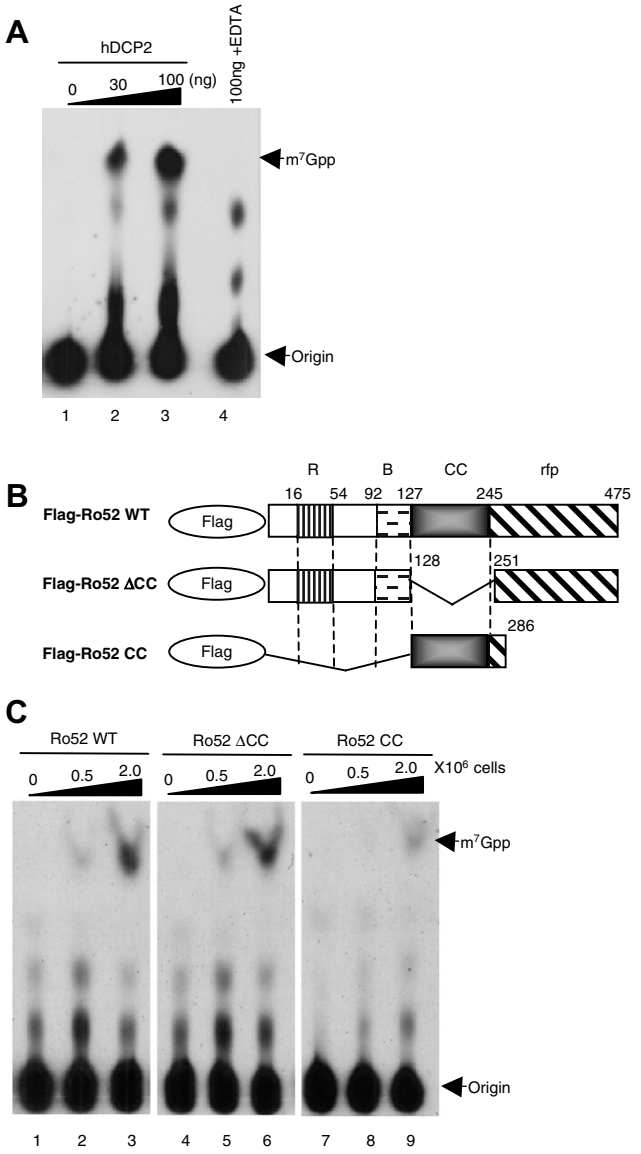

Fig. 3. Decapping assay by recombinant hDCP2 with Ro52 or deletion mutants of Ro52. (A) The assay was carried out using 0, 30 or 100 ng of bacterially expressed 6xHis-tagged hDCP2 with cap labeled β-actin mRNA substrate in the absence (lanes 1–3) or presence of EDTA (lanes 4). The reaction products were resolved by TLC. Migration of standard was shown at right. (B) Schematic representation of Flag-tagged Ro52. Each region or domain is described in Fig. 2A. (C) The assay was carried out using 10 ng of bacterially expressed 6xHis-tagged hDCP2 with cap labeled β-actin mRNA substrate and immunopurified Flag-tagged Ro52 WT (lanes 1–3 corresponding to 0, 0.5×10^6, 2×10^6 cell-worth of proteins, respectively) or its deletion mutants, Ro52 ΔCC (lanes 4–6 corresponding to 0, 0.5×10^6, 2×10^6 cell-worth of proteins, respectively) or Ro52 CC (lanes 7–9 corresponding to 0, 0.5×10^6, 2×10^6 cell-worth of proteins, respectively). The reaction products were resolved by TLC. Migration of standard was shown at right.

Discussion

In the present study, we showed that the autoantigen SSA/Ro52 protein is associated with mRNA-decapping enzyme hDCP2, with the N-terminal and C-terminal domains of Ro52 being required for its binding to hDCP2, and the N-terminal and C-terminal domains of hDCP2 being required for its binding to Ro52. Furthermore, hDCP2 enzymatic activity is enhanced by its interaction with Ro52.

To examine the biochemical interactions between the two proteins, we initially tried to demonstrate endogenous association with the use of coimmunoprecipitation assay. However, Western blotting with commercially available anti-hDCP2 antibodies did not detect endogenous hDCP2 in 1 mg of total cell lysates of 293 FT or HeLa cell lines (data not shown), although these were reported to contain endogenous hDCP2 protein [16,17]. Moreover, we observed that Ro52 bound to immunoglobulin G (data not shown), as described previously [30]. These data implied that the presently available anti-hDCP2 antibody was inadequate for detecting endogenous hDCP2 protein in coimmunoprecipitation assay, and that the binding of Ro52 to hDCP2 may be observed in a nonspecific manner by immunoprecipitation assay. We therefore conducted GST pull-down assay using GST-hDCP2 protein expressed in mammalian cells. Moreover, to exclude nonspecific binding in GST-glutathione beads system, we further confirmed the biochemical interaction by using a biotin pull-down system with avidin beads. These biochemical assays demonstrated binding of Ro52 to hDCP2 and determined the binding domains involved in the specific Ro52-hDCP2 interaction. However, we could not formally exclude the possibility that other components involved in p-bodies, such as hDCP1 and GW182, were associated directly or indirectly with the Ro52-hDCP2 interaction. Moreover, since Ro52 and hDCP2 contain binding domains for nucleic acids [31,32], it is also possible that RNA itself mediates the association of Ro52 and hDCP2 in p-bodies.

The above data that Ro52 interaction with hDCP2 lead the notion that the decapping activity of hDCP2 may be affected by association with Ro52. As shown in Fig. 3, our *in vitro* decapping assay system to directly examine Ro52-associated decapping activity of hDCP2 revealed that Ro52 enhanced decapping activity in a dose-dependent manner. We also found that the interaction between Ro52 and hDCP2 played an important role in enhancing Ro52-induced hDCP2 decapping activity (Fig. 3). These results therefore suggested that Ro52 is involved in mRNA metabolism in a given circumstance. Translocation of Ro52 was observed in p-bodies-like perinuclear discrete speckled patterns, and was associated with enhanced IL-2 production following CD28 stimulation [10]. In addition, expression of inflammatory cytokines such as TNFα was regulated by the mRNA-decapping protein Tristetrapro-

lin (TTP) [16], which may interact with hDCP1 and hDCP2 in T cells to enhance decapping activity. We therefore speculate that Ro52 in T cell may be associated with production of such cytokines as IL-2 by regulating decapping activity in response to CD28 stimulation.

Our data have thus identified the major autoantigen Ro52 as a protein capable of interacting with and regulating the activity of hDCP2 in p-bodies, providing a novel evidence demonstrating an association between mRNA decay and autoimmune diseases.

Acknowledgments

We thank Dr. Bertrand Seraphin for pEGFP-hDCP2 plasmid, Dr. Megerdith Kiledjian for pET-hDCP2 ΔN93 and pET-hDCP2. We are greatly indebted to Mr. Yoshiaki Itoh for his technical assistance and to Dr. Nam H. Dang for English proofs.

T.Y., K.O., and C.M. are recipients of a Grant-in-Aid of the Ministry of Education, Science, Sports and Culture.

References

[1] M.A. Alspaugh, E.M. Tan, Antibodies to cellular antigens in Sjogren's syndrome, J. Clin. Invest. 55 (1975) 1067–1073.
[2] M.D. Rader, C. O'Brien, Y.S. Liu, J.B. Harley, M. Reichlin, Heterogeneity of the Ro/SSA antigen. Different molecular forms in lymphocytes and red blood cells, J. Clin. Invest. 83 (1989) 1293–1298.
[3] S.L. Deutscher, J.B. Harley, J.D. Keene, Molecular analysis of the 60-kDa human Ro ribonucleoprotein, Proc. Natl. Acad. Sci. USA 85 (1988) 9479–9483.
[4] E.K. Chan, F. Di Donato, J.C. Hamel, C.E. Tseng, J.P. Buyon, 52-kD SS-A/Ro: genomic structure and identification of an alternatively spliced transcript encoding a novel leucine zipper-minus autoantigen expressed in fetal and adult heart, J. Exp. Med. 182 (1995) 983–992.
[5] A. Reymond, G. Meroni, A. Fantozzi, G. Merla, S. Cairo, L. Luzi, D. Riganelli, E. Zanaria, S. Messali, S. Cainarca, A. Guffanti, S. Minucci, P.G. Pelicci, A. Ballabio, The tripartite motif family identifies cell compartments, EMBO J. 20 (2001) 2140–2151.
[6] E.K. Chan, J.C. Hamel, J.P. Buyon, E.M. Tan, Molecular definition and sequence motifs of the 52-kD component of human SS-A/Ro autoantigen, J. Clin. Invest. 87 (1991) 68–76.
[7] E. Ben-Chetrit, E.K. Chan, K.F. Sullivan, E.M. Tan, A 52-kD protein is a novel component of the SS-A/Ro antigenic particle, J. Exp. Med. 167 (1988) 1560–1571.
[8] J.B. Harley, E.L. Alexander, W.B. Bias, O.F. Fox, T.T. Provost, M. Reichlin, H. Yamagata, F.C. Arnett, Anti-Ro (SS-A) and anti-La (SS-B) in patients with Sjogren's syndrome, Arthritis Rheum. 29 (1986) 196–206.
[9] T. Dorner, E. Feist, C. Held, K. Conrad, G.R. Burmester, F. Hiepe, Differential recognition of the 52-kd Ro(SS-A) antigen by sera from patients with primary biliary cirrhosis and primary Sjogren's syndrome, Hepatology 24 (1996) 1404–1407.
[10] T. Ishii, K. Ohnuma, A. Murakami, N. Takasawa, T. Yamochi, S. Iwata, M. Uchiyama, N.H. Dang, H. Tanaka, C. Morimoto, SS-A/Ro52 an autoantigen involved in CD28-mediated IL-2 production, J. Immunol. 170 (2003) 3653–3661.
[11] J.H. Yu, W.H. Yang, T. Gulick, K.D. Bloch, D.B. Bloch, Ge-1 is a central component of the mammalian cytoplasmic mRNA processing body, RNA 11 (2005) 1795–1802.
[12] T. Eystathioy, C.L. Peebles, J.C. Hamel, J.H. Vaughn, E.K. Chan, Autoantibody to hLSm4 and the heptameric LSm complex in anti-Sm sera, Arthritis Rheum. 46 (2002) 726–734.
[13] T. Eystathioy, E.K. Chan, K. Takeuchi, M. Mahler, L.M. Luft, D.W. Zochodne, M.J. Fritzler, Clinical and serological associations of autoantibodies to GW bodies and a novel cytoplasmic autoantigen GW182, J. Mol. Med. 81 (2003) 811–818.
[14] R.A. Bhanji, T. Eystathioy, E.K. Chan, D.B. Bloch, M.J. Fritzler, Clinical and serological features of patients with autoantibodies to GW/P bodies, Clin. Immunol. 125 (2007) 247–256.
[15] E. van Dijk, N. Cougot, S. Meyer, S. Babajko, E. Wahle, B. Seraphin, Human Dcp2: a catalytically active mRNA decapping enzyme located in specific cytoplasmic structures, EMBO J. 21 (2002) 6915–6924.
[16] M. Fenger-Gron, C. Fillman, B. Norrild, J. Lykke-Andersen, Multiple processing body factors and the ARE binding protein TTP activate mRNA decapping, Mol. Cell 20 (2005) 905–915.
[17] N. Cougot, S. Babajko, B. Seraphin, Cytoplasmic foci are sites of mRNA decay in human cells, J. Cell Biol. 165 (2004) 31–40.
[18] U. Sheth, R. Parker, Decapping and decay of messenger RNA occur in cytoplasmic processing bodies, Science 300 (2003) 805–808.
[19] T. Eystathioy, A. Jakymiw, E.K. Chan, B. Seraphin, N. Cougot, M.J. Fritzler, The GW182 protein colocalizes with mRNA degradation associated proteins hDcp1 and hLSm4 in cytoplasmic GW bodies, RNA 9 (2003) 1171–1173.
[20] D. Ingelfinger, D.J. Arndt-Jovin, R. Luhrmann, T. Achsel, The human LSm1-7 proteins colocalize with the mRNA-degrading enzymes Dcp1/2 and Xrnl in distinct cytoplasmic foci, RNA 8 (2002) 1489–1501.
[21] C. Fillman, J. Lykke-Andersen, RNA decapping inside and outside of processing bodies, Curr. Opin. Cell Biol. 17 (2005) 326–331.
[22] T. Dunckley, R. Parker, The DCP2 protein is required for mRNA decapping in *Saccharomyces cerevisiae* and contains a functional MutT motif, EMBO J. 18 (1999) 5411–5422.
[23] J. Lykke-Andersen, Identification of a human decapping complex associated with hUpf proteins in nonsense-mediated decay, Mol. Cell Biol. 22 (2002) 8114–8121.
[24] K. Ohnuma, T. Yamochi, M. Uchiyama, K. Nishibashi, N. Yoshikawa, N. Shimizu, S. Iwata, H. Tanaka, N.H. Dang, C. Morimoto, CD26 up-regulates expression of CD86 on antigen-presenting cells by means of caveolin-1, Proc. Natl. Acad. Sci. USA 101 (2004) 14186–14191.
[25] T. Yamochi, I. Nishimoto, T. Okuda, M. Matsuoka, ik3-1/Cables is associated with Trap and Pctaire2, Biochem. Biophys. Res. Commun. 286 (2001) 1045–1050.
[26] N. Pourmand, I. Blange, N. Ringertz, I. Pettersson, Intracellular localisation of the Ro 52 kD auto-antigen in HeLa cells visualised with green fluorescent protein chimeras, Autoimmunity 28 (1998) 225–233.
[27] T. Eystathioy, E.K. Chan, S.A. Tenenbaum, J.D. Keene, K. Griffith, M.J. Fritzler, A phosphorylated cytoplasmic autoantigen, GW182, associates with a unique population of human mRNAs within novel cytoplasmic speckles, Mol. Biol. Cell 13 (2002) 1338–1351.
[28] D. Teixeira, U. Sheth, M.A. Valencia-Sanchez, M. Brengues, R. Parker, Processing bodies require RNA for assembly and contain nontranslating mRNAs, RNA 11 (2005) 371–382.
[29] S. Zhang, C.J. Williams, M. Wormington, A. Stevens, S.W. Peltz, Monitoring mRNA decapping activity, Methods 17 (1999) 46–51.
[30] Y. Yang, T. Eversole, D.J. Lee, R.D. Sontheimer, J.D. Capra, Protein–protein interactions between native Ro52 and immunoglobulin G heavy chain, Scand. J. Immunol. 49 (1999) 620–628.
[31] C. Piccirillo, R. Khanna, M. Kiledjian, Functional characterization of the mammalian mRNA decapping enzyme hDcp2, RNA 9 (2003) 1138–1147.
[32] M.B. Frank, Characterization of DNA binding properties and sequence specificity of the human 52 kDa Ro/SS-A (Ro52) zinc finger protein, Biochem. Biophys. Res. Commun. 259 (1999) 665–670.